

Dynamical modelling of disc vertical structure in superthin galaxy ‘UGC 7321’ in braneworld gravity: An MCMC study

K. Aditya^{1,*}, Indrani Banerjee^{2,†}, Arunima Banerjee^{1,‡} and Soumitra Sengupta^{2,§}

¹ Department of Physics, Indian Institute of Science Education and Research (IISER) Tirupati, Tirupati - 517507, India

² School of Physical Sciences, Indian Association for the Cultivation of Science, 2A & 2B Raja S. C. Mullick Road, Kolkata-700032, India

29 September 2020

ABSTRACT

Low surface brightness (LSBs) superthins constitute classic examples of very late-type galaxies, with their disc dynamics strongly regulated by their dark matter halos. In this work we consider a gravitational origin of dark matter in the brane world scenario, where the higher dimensional Weyl stress term projected onto the 3-brane acts as the source of dark matter. In the context of the braneworld model, this dark matter is referred to as the ‘dark mass’. This model has been successful in reproducing the rotation curves of several low surface brightness and high surface brightness galaxies. Therefore it is interesting to study the prospect of this model in explaining the vertical structure of galaxies which has not been explored in the literature so far. Using our 2-component model of gravitationally-coupled stars and gas in the external force field of this *dark mass*, we fit the observed scale heights of stellar and atomic hydrogen (HI) gas of superthin galaxy ‘UGC7321’ using the Markov Chain Monte Carlo approach. We find that the observed scaleheights of ‘UGC7321’ can be successfully modelled in the context of the braneworld scenario. In addition, the model predicted rotation curve also matches the observed one. The implications on the model parameters are discussed.

1 INTRODUCTION

Historically, the concept of dark matter was invoked to address the missing mass problem in spiral galaxies (Rubin et al. 1979) as well as to explain the mass discrepancy in galaxy clusters (Zwicky 1937, 1933). The observed rotation curves of galaxies, as determined by optical tracers or by HI 21cm radio-synthesis studies, are flat or tend to be asymptotically flat. Interestingly, however, the observed distribution of visible matter predicts a Keplerian fall-off beyond the visible galactic disc (Binney & Tremaine 2008). Basic physics suggests, the flatness of the rotation curve requires the total galactic mass to be increasing linearly with galactocentric radius even beyond the baryonic disc of the galaxy. This hinted at the presence of non-luminous matter in the discs of galaxies, the “dark matter”, which was invoked to explain the mass discrepancy and hence the flat rotation curves of spiral galaxies. In fact, the “dark matter” has been used to explain the observed rotation curves of a wide range of spiral galaxies including massive high surface brightness galaxies (HSBs), intermediate-mass low surface brightness galaxies (LSBs) to dwarf irregulars (Sofue & Rubin 2001; McGaugh et al. 2001; Kranz et al. 2003; Gentile et al. 2004; de Blok 2005; de Blok et al. 2008; Oh et al. 2015). Similarly, the concept of “dark matter” came as a rescue to address the mass discrepancy problem in galaxy clusters. The mass

of a galaxy cluster estimated by summing up the masses of its individual member galaxies is much lower than the virial mass of the galaxy-cluster determined using the observed line of sight velocity dispersion values of the member galaxies (Carlberg et al. 1997). This again hinted at the presence of non-luminous matter at cluster scales, which could be explained by invoking the concept of “dark matter”.

Although the “dark matter” is generally thought to resolve a host of astrophysical and cosmological problems, the fundamental particles constituting the dark matter have evaded detection in dark matter search experiments (See, for example, Cryogenic Dark Matter Search (CDMS), Agnese et al. (2013)). The lack of detectional evidence for dark matter particles as well as a large number of problems arising in the dark-matter particle approach (Peebles & Nusser 2010), (Kroupa 2012, 2015), (Pawlowski et al. 2015) opens up the possibility for a gravitational origin of dark matter wherein Newtonian gravity is modified to explain the ‘missing mass’ problem.

One of the earliest attempts to modify the Newton’s laws for explaining the galactic rotation curves was Modified Newtonian dynamics (MOND) (Milgrom 1983), which is well-tested in the context of the Milky Way (Famaey & Binney 2005) and also on a large sample of spiral galaxies (de Blok & McGaugh 1998; Sanders & Verheijen 1998; Sanders & Noordermeer 2007). Besides, extra dimensional

models or brane-worlds can also lead to alternative gravitational origin of “dark matter” (Binetruy et al. 2000; Csaki et al. 1999; Mazumdar 2001; Maartens 2000, 2004a; Koyama 2003; Haghani et al. 2012) where the Standard Model particles and fields are confined in a 3-brane while gravity enters into the bulk (Antoniadis 1990; Antoniadis et al. 1998; Arkani-Hamed et al. 1998; Randall & Sundrum 1999b; Garriga & Tanaka 2000; Randall & Sundrum 1999a; Csaki et al. 2000), (see Fichet (2020) and references therein for braneworld models with matter fields not localized onto the brane). Higher dimensional models or brane-worlds were mainly introduced to provide a scheme to unify all the known forces of nature thereby giving birth to string theory and eventually M-theory (Kaluza 2018; Klein 1926; Horava & Witten 1996; Polchinski 1998). The huge difference between the Planck scale and the electroweak scale led to the gauge hierarchy problem in particle physics which could also be addressed by introducing higher dimensions (Antoniadis 1990; Arkani-Hamed et al. 1998; Antoniadis et al. 1998; Randall & Sundrum 1999a; Csaki et al. 2000). Further, extra-dimensional models have interesting phenomenological (Arkani-Hamed et al. 1999; Davoudiasl et al. 2000b,a, 2001; Hundi & SenGupta 2013; Chakraborty & SenGupta 2014) and cosmological implications (Dienes et al. 1999; Lukas et al. 2000; Arkani-Hamed et al. 2000; Mazumdar & Wang 2000; Chakraborty & Sengupta 2014; Banerjee & Paul 2017; Banerjee et al. 2019). Moreover, since the nature of gravity in the high energy regime is unknown, it is often believed that the deviations from Einstein gravity may manifest itself through the existence of extra dimensions.

The brane world model of Maartens (2004b) considers a single 3-brane embedded in a five dimensional bulk. The modifications in the Einstein’s equations arise mainly due to the non-local effects of the bulk Weyl tensor. A brane observer perceives this Weyl stress term like a fluid, known as the Weyl fluid, with its own energy density and pressure. It was shown by Mak & Harko (2004), Harko & Cheng (2006), Boehmer & Harko (2007), Rahaman et al. (2008) and Gergely et al. (2011b) that such a model successfully complies with observed rotation curves of galaxies. The aim of this work is to explore the prospect of the brane world model in explaining the observed scale height of stars and neutral hydrogen gas (HI) in galaxies. Towards this end, we consider the prototypical low surface brightness superthin galaxy, UGC7321, which was found to be dark matter dominated at all radii (Banerjee et al. 2010). In fact, Banerjee & Jog (2013) have shown that the superthin vertical structure of the stellar disc crucially depends on its dense and compact dark matter halo. Therefore, in this work, we intend to constrain its dark matter density profile in the brane world scenario using the observed stellar and HI scale heights of UGC 7321. We derive the density profile of the Weyl fluid which arises in the brane world scenario to resemble the cored dark matter halo profile consistent with mass models of the low surface brightness galaxies (de Blok 2005). We use this derived density profile of the Weyl fluid to mimic the dark matter density profile in the 2-component model of gravitationally-coupled stars and gas in the external force field of the dark matter halo (Narayan & Jog 2002). The observed stellar and HI scale heights are used to constrain the vertical stellar velocity dispersion and vertical HI velocity dispersion of the galactic disc in addition to the Weyl

parameters. Finally, we check the consistency of the Weyl model with the observed rotation curve of UGC 7321.

The paper is organised as follows: in §2, we describe the brane-world model and present the density profile derived from such a model mimicking the characteristics of the dark matter. In §3, we present the 2-component model of the baryonic disc in the force field of the dark matter halo such that the Weyl fluid plays the role of the dark matter. We present our results in the context of the the LSB super thin galaxy UGC 7321 in §4 and conclude with a summary of our findings in §5.

2 BRANEWORLD GRAVITY: A POSSIBLE PROXY TO DARK MATTER

We consider a single 3-brane embedded in a 5-D spacetime (the bulk). We assume that the Standard Model particles and fields are confined in the brane while gravity permeates the extra dimensions. The coordinates of the bulk are denoted by latin indices x^a , $a = 0, 1, \dots, 4$ while the brane coordinates are denoted by Greek indices x^μ , $\mu = 0, 1, 2, 3$.

We consider Einstein gravity in the bulk described by the action,

$$S_{bulk} = \int d^5x \sqrt{-\tilde{g}} \left[\frac{R}{2\kappa_5^2} + \Lambda_5 + \delta(\phi)\mathcal{L}_m \right] \quad (1)$$

where \tilde{g} is the determinant of the bulk metric \tilde{g}_{ab} , R is the bulk Ricci scalar, $\kappa_5^2 = 8\pi G_5$ is the five dimensional gravitational constant, Λ_5 is the bulk cosmological constant and \mathcal{L}_m is the matter Lagrangian in the brane representing standard model fields.

From the action (given by 1) the gravitational field equations in the bulk are given by,

$$R_{ij} - \frac{1}{2}G_{ij}R = \kappa_5^2 T_{ij} \quad (2)$$

where R_{ij} is the bulk Ricci tensor and T_{ij} the energy-momentum in the bulk. The bulk energy-momentum tensor can be written as,

$$T_{ab} = -\Lambda_5 G_{ab} + \delta(\phi)(-\lambda_T g_{\mu\nu} + \tau_{\mu\nu}) e_a^\mu e_b^\nu \quad (3)$$

where ϕ refers to the extra coordinate, the brane being located at $\phi = 0$ and e_a^μ projects the quantities of the bulk onto the brane. The induced metric on the $\phi = 0$ time-like hypersurface is denoted by $g_{\mu\nu}$. The negative vacuum energy density on the bulk Λ_5 , the brane tension λ_T and the brane energy-momentum tensor $\tau_{\mu\nu}$ are the sources of the gravitational field on the bulk.

In this work we adopt the 3+1+1 covariant approach in brane worlds developed in Keresztes & Gergely (2010a,b). In this formalism, first the space-like extra coordinate ϕ is singled out and the 5-D spacetime is foliated by a family of 4-D time-like $\phi = \text{constant}$ hypersurfaces, where the hypersurface designated by $\phi = 0$ represents the brane. Next, in the 4-D time-like hypersurfaces the time coordinate is singled out and the 4-D spacetime is foliated in terms of the 3-D space-like $t = \text{constant}$ hypersurfaces. The propagation along the extra-dimension and the temporal direction are associated with the integral curves $n^a = \frac{dx^a}{d\phi}$ and $u^a = \frac{dx^a}{dt}$ respectively, obeying the normalization conditions $1 = n^a n_a = -u^b u_b$ and

the perpendicularity condition $n^c u_c = 0$. The bulk metric \tilde{g}_{ab} is connected to the brane metric g_{ab} by the relation,

$$\tilde{g}_{ab} = g_{ab} + n_a n_b \quad (4)$$

It can be shown that the 5-D covariant derivative (denoted by $\tilde{\nabla}$) of u^a and n^a can be expressed in terms of several kinematic quantities, involving three scalars, four three-vectors and a symmetric, trace-free three-tensor, of which two scalars and one of the three vectors arise in common during the decomposition of both $\tilde{\nabla}_a u_b$ and $\tilde{\nabla}_a n_b$ (Keresztes & Gergely 2010b). Further, the 5-D Weyl tensor \tilde{C}_{abcd} can be decomposed into several gravito-electro-magnetic quantities (involving scalars, vectors and tensors) which carry distinct geometrical meaning (Keresztes & Gergely 2010b).

Gauss-Codazzi equations which relate the Riemann tensor of the bulk to that of the brane by means of the projectors and the extrinsic curvature tensor are used to arrive at the effective four dimensional gravitational field equations. The extrinsic curvature $K_{\mu\nu}$, which encodes the embedding of the brane into the bulk is associated with the covariant derivative of the normalized normals to the brane n^a . If the brane has an energy momentum tensor, the extrinsic curvature $K_{\mu\nu}$ exhibits a discontinuity across the brane. This discontinuity in the extrinsic curvature is related to the brane energy momentum tensor by means of Israel junction conditions and a symmetrical brane embedding (Z_2 symmetry) (Keresztes & Gergely 2010b; Chakraborty & SenGupta 2015)

With the above considerations the effective four-dimensional gravitational field equations on the brane assume the form,

$$\mathcal{R}_{\mu\nu} - \frac{1}{2}\mathcal{R}g_{\mu\nu} = -\Lambda_4 g_{\mu\nu} + 8\pi G_4 \tau_{\mu\nu} + \kappa_5^4 \pi_{\mu\nu} - E_{\mu\nu} \quad (5)$$

where

$$\Lambda_4 = \frac{1}{2}\kappa_5^2 \left[\Lambda_5 + \frac{1}{6}\kappa_5^2 \lambda_T^2 \right] \quad (6)$$

$$G_4 = \frac{\kappa_5^4 \lambda_T}{48\pi} \quad (7)$$

$$\pi_{\mu\nu} = -\frac{1}{4}\tau_{\mu\alpha}\tau_\nu^\alpha + \frac{1}{12}\tau\tau_{\mu\nu} + \frac{1}{8}g_{\mu\nu}\tau_{\alpha\beta}\tau^{\alpha\beta} - \frac{1}{24}g_{\mu\nu}\tau^2 \quad (8)$$

$$E_{\mu\nu} = \tilde{C}_{abcd}e_\mu^a n^b e_\nu^c n^d \quad (9)$$

In 5, Λ_4 and G_4 represent the 4-dimensional cosmological constant and gravitational constant respectively while $\mathcal{R}_{\mu\nu}$ and \mathcal{R} refer to the Ricci tensor and Ricci scalar on the brane. The local effects of the bulk on the brane is encoded in the term $\pi_{\mu\nu}$ while $E_{\mu\nu}$, the electric part of the bulk Weyl tensor \tilde{C}_{abcd} captures the non-local effect from the free bulk gravitational field. In 6 the brane tension can be adjusted with the bulk cosmological constant to yield de-Sitter, anti de-Sitter or flat branes such that it serves as the fine balancing relation of the Randall-Sundrum single brane model (Randall & Sundrum 1999b; Shiromizu et al. 2000). The conservation of the matter energy-momentum tensor on the brane enables us to constrain $E_{\mu\nu}$ and $\pi_{\mu\nu}$ as $D_\nu E_\mu^\nu - \kappa_5^4 D_\nu \pi_\mu^\nu = 0$, (where D_ν represents the brane covariant derivative).

The symmetry properties of the trace-free tensor $E_{\mu\nu}$ allow an irreducible decomposition of the tensor in terms of a given 4-velocity field u^μ (Maartens 2001; Harko & Mak

2004),

$$E_{\mu\nu} = -k^4 \left[U(r)(u_\mu u_\nu + \frac{1}{3}\zeta_{\mu\nu}) + 2Q_{(\mu} u_{\nu)} + P_{\mu\nu} \right] \quad (10)$$

where $\zeta_{\mu\nu} = g_{\mu\nu} + u_\mu u_\nu$ is the induced metric associated with the 3-D space-like hypersurfaces orthogonal to u^μ , $k = \frac{\kappa_5}{\kappa_4}$ and $\kappa_4^2 = 8\pi G_4$. It is important to note that $\kappa_4^2 = \kappa_5^4 \lambda_T / 6$ and we retrieve general relativity in the limit $\lambda_T^{-1} \rightarrow 0$ ((Harko & Mak 2004)). The scalar $U(r) = -\frac{1}{k^4} E_{\mu\nu} u^\mu u^\nu$ in 10 is often known as the ‘‘Dark Radiation’’ term, while $Q_\mu = \frac{1}{k^4} \zeta_\mu^\alpha E_{\alpha\beta} u^\beta$ represents a spatial vector and $P_{\mu\nu} = -\frac{1}{k^4} [\zeta_{(\mu}^\alpha \zeta_{\nu)}^\beta - \frac{1}{3}\zeta_{\mu\nu}\zeta^{\alpha\beta}] E_{\alpha\beta}$ consists of a spatial, tracefree, symmetric tensor.

Our goal in this work is to explain observations at the galactic scale, namely, the vertical scaleheight of stars and gas and the rotation curves of galaxies in the framework of braneworld gravity. We have already noted that in such a scenario, the bulk geometry induces an effective energy-momentum tensor ($E_{\mu\nu}$) on the brane which can play the crucial role of dark matter. The effect of baryons on the brane geometry is neglected and therefore we take $\tau_{\mu\nu} = \pi_{\mu\nu} = 0$.

As a result the gravitational field equations on the brane (given by 5) reduce to,

$$\mathcal{R}_{\mu\nu} - \frac{1}{2}\mathcal{R}g_{\mu\nu} = -\Lambda_4 g_{\mu\nu} - E_{\mu\nu} \quad (11)$$

The conservation of energy-momentum tensor on the brane then assumes the form $D_\nu E_\mu^\nu = 0$. Moreover, the mass distribution of the dark matter can be approximately taken to be spherically symmetric and time-independent, and as a result we take $Q_\mu = 0$ in 10 such that $D_\nu E_\mu^\nu = 0$ leads to,

$$\frac{1}{3}\bar{D}_\mu U + \frac{4}{3}U A_\mu + \bar{D}^\nu P_{\nu\mu} + A^\nu P_{\nu\mu} = 0 \quad (12)$$

where $A_\mu = u^\nu D_\nu u_\mu$ is the acceleration and \bar{D} denotes covariant derivative on the space-like hypersurface associated with the metric $\zeta_{\mu\nu}$ orthonormal to u_μ . Further, assumption of spherical symmetry, enables us to write $A_\mu = A(r)r_\mu$, while the term $P_{\mu\nu}$ takes the form,

$$P_{\mu\nu} = P(r) \left(r_\mu r_\nu - \frac{1}{3}\zeta_{\mu\nu} \right) \quad (13)$$

where $A(r)$ and $P(r)$ (also known as the ‘‘Dark Pressure’’) are scalar functions of the radial coordinate r and r_μ is the unit radial vector. In what follows we will derive static and spherically symmetric solution of 11.

2.1 Motion of test particles in the braneworld model

In this work we are interested in exploring the properties of low surface brightness galaxies (LSBs) where the dark matter halo dominates the disc dynamics even in the inner galaxy where the baryonic disc is present. (Gergely et al. 2011a; De Blok et al. 2001; Banerjee et al. 2010; Banerjee & Bapat 2017). Therefore, a static and spherically symmetric spacetime is used to describe the brane metric and one can neglect the effect of the cylindrically symmetric baryonic disk on the brane geometry.

In the last section, we noted that the presence of extra dimensions endows an effective energy-momentum tensor on

the brane $E_{\mu\nu}$ due to the non-local effects of the bulk Weyl tensor. This Weyl stress term essentially plays the role of dark matter in this work. Since LSBs are dark matter dominated, one can neglect the effect of the cylindrically symmetric baryonic disk on the brane geometry such that a static and spherically symmetric spacetime is used to describe the brane metric,

$$ds^2 = -e^{\nu(r)} dt^2 + e^{\lambda(r)} dr^2 + r^2(d\theta^2 + \sin^2\theta d\phi^2) \quad (14)$$

We solve for $\nu(r)$, $\lambda(r)$, $U(r)$ and $P(r)$ from the fact that 14 satisfies 11 and 12.

By studying the motion of test particles in the above spacetime it can be shown that the tangential velocity or the circular velocity of motion is given by

$$v_c^2 = \frac{r\nu'}{2} \quad (15)$$

(Gergely et al. 2011b)

With 14 the gravitational field equations and the energy momentum tensor conservation in the brane gives us,

$$-e^{-\lambda} \left(\frac{1}{r^2} - \frac{\lambda'}{r} \right) + \frac{1}{r^2} = 3\alpha U \quad (16)$$

$$e^{-\lambda} \left(\frac{\nu'}{r} + \frac{1}{r^2} \right) - \frac{1}{r^2} = \alpha(U + 2P) \quad (17)$$

$$\frac{e^{-\lambda}}{2} \left(\nu'' + \frac{\nu'^2}{2} + \frac{\nu' - \lambda'}{r} - \frac{\nu' \lambda'}{2} \right) = \alpha(U - P) \quad (18)$$

$$\nu' = -\frac{U' + 2P'}{2U + P} - \frac{6P}{(2U + P)r} \quad (19)$$

where prime denotes derivative with respect to r and $\alpha = \frac{1}{4\pi G_4 \lambda_T}$. One can show that the solution of these equations lead to the following form for $e^{-\lambda}$,

$$e^{-\lambda} = 1 - \frac{\Lambda_4}{3} r^2 - \frac{Q(r)}{r} - \frac{C}{r} \quad (20)$$

where $C = 2GM$ (M being the baryonic mass) and $Q(r)$ is defined as,

$$Q(r) = \frac{3}{4\pi G_4 \lambda_T} \int r^2 U(r) dr \quad (21)$$

(Gergely et al. 2011b). From the form of $e^{-\lambda}$ it can be inferred that $Q(r)$ is the gravitational mass originating from the dark radiation and can be interpreted as the ‘‘dark mass’’ term.

Further, one can show that for a static, spherically symmetric spacetime the ordinary differential equations for dark radiation $U(r)$ and dark pressure $P(r)$ satisfy ,

$$\frac{dU}{dr} = -2 \frac{dP}{dr} - 6 \frac{P}{r} - \frac{(2U + P)[2G_4 M + Q + \{\alpha(U + 2P + \frac{2}{3}\chi)\}r^3]}{r^2(1 - \frac{2G_4 M}{r} - \frac{Q(r)}{r} - \frac{\chi}{3}r^2)} \quad (22)$$

and

$$\frac{dQ}{dr} = 3\alpha r^2 U. \quad (23)$$

where $\alpha = \frac{1}{4\pi G_4 \lambda_T}$ and $\chi = -\Lambda_4$ (Gergely et al. 2011b). In the subsequent calculations we will neglect the effect of the cosmological constant Λ_4 (Gergely et al. 2011b) on the vertical scale height of the galaxies, i.e. we will take $\chi = -\Lambda_4 = 0$. Since the observed cosmological constant required to explain

the accelerated expansion of the universe is extremely small ($\Lambda_4 \approx 10^{-52} \text{m}^{-2}$ or 10^{-122} in Planckian units), its effect on the mass energy of the galaxy can be ignored as being several orders of magnitude smaller than the observed masses.

22 and 23 can be recast into a more convenient form namely,

$$\frac{d\mu}{d\theta} = -(2\mu + p) \frac{\tilde{q} + \frac{1}{3}(\mu + 2p)}{1 - \tilde{q}} - 2 \frac{dp}{d\theta} + 2\mu - 2p \quad (24)$$

$$= -2v_{tg}^2(2\mu + p) - 2 \frac{dp}{d\theta} + 2\mu - 2p$$

$$\frac{d\tilde{q}}{d\theta} = \mu - \tilde{q} \quad (25)$$

by defining the variables,

$$\tilde{q} = \frac{2G_4 M + Q}{r}; \quad \mu = 3\alpha r^2 U; \quad p = 3\alpha r^2 P; \quad \theta = \ln r; \quad (26)$$

24 and 25 can be referred to as the differential equations governing the source terms on the brane, while the circular velocity of the test particle v_c assumes the form,

$$v_c^2 = \frac{1}{2} \frac{\tilde{q} + \frac{1}{3}(\mu + 2p)}{1 - \tilde{q}} \quad (27)$$

2.2 Choice of the equation of state of the Weyl fluid

The brane observer perceives the extra dimensions through the term $E_{\mu\nu}$ which in turn can be written in terms of the dark radiation $U(r)$ and the dark pressure $P(r)$. These are like the energy density and the pressure of the stress energy tensor of the Weyl fluid whose origin is attributed to extra dimensions. An equation of state connecting the dark radiation U and dark pressure P is therefore necessary since the source equations 24 and 25 cannot be solved simultaneously until we impose some further conditions on them. Hence, we choose some specific relations between dark radiation U and dark pressure P , necessarily defining the various equations of state in the framework of the brane world model.

In order to close the system of field equations 24 and 25, we adopt the 3+1+1 covariant approach developed in Keresztes & Gergely (2010a,b), also discussed briefly in 2. This approach is quite different from the full 5-D approach used in Wiseman (2002) where the five dimensional Einstein’s equations were numerically solved assuming that the matter localized in the brane is associated with a static and spherically symmetric configuration. Such a choice of matter distribution on the brane was considered since Wiseman (2002) aimed at explaining observations related to stars confined in the brane. In order to obtain a regular bulk metric Wiseman (2002) assumed a density profile resembling a deformed top-hat function which resulted in a regular bulk geometry with axial symmetry. Our aim on the other hand, is to explain observations at the galactic scale where the bulk geometry plays the vital role of dark matter through the term $E_{\mu\nu}$.

In order to proceed further we consider the following assumptions: (i) no matter in the brane (the effect of baryons on the brane metric is neglected), (ii) fine-tuning on the brane (i.e. $\Lambda_4 = 0$), (iii) cosmological vacuum in the 5-D spacetime, (iv) symmetrical embedding on the brane (Z_2

symmetry) and (v) the brane spacetime is static and spherically symmetric, such that the brane metric assumes the form 14.

From the above assumptions it can be shown that the only non-zero kinematical quantity associated with the temporal normal u^μ is the acceleration $A_\mu = u^\nu D_\nu u_\mu$ (Gergely et al. 2011a). Since we are interested in static and spherically symmetric solutions Q_μ in 10 vanishes and the requirement of spherical symmetry ensures that the brane spacetime can be further decomposed into a 2+1+1 form such that $A_\mu = A(r)r_\mu$ and $P_{\mu\nu}$ in 10 can be written as 13, where $A(r)$ and $P(r)$ (also known as the ‘‘Dark Pressure’’) are scalar functions of the radial coordinate r . Due to spherical symmetry the electric part of the 4-D Weyl tensor $\tilde{E}_{\mu\nu} = C_{\alpha\mu\beta\nu}u^\alpha u^\beta$ ($C_{\alpha\mu\beta\nu}$ being the 4-D Weyl tensor) can be further reduced in the form,

$$\tilde{E}_{\mu\nu} = \tilde{E}(r)\left(r_\mu r_\nu - \frac{\zeta_{\mu\nu}}{3}\right) \quad (28)$$

Moreover, we have the kinematical scalar $\tilde{\Theta}(r) = \bar{D}_a r^a$ associated with the expansion of the radial geodesics in the $t = \text{constant}$ hypersurfaces.

The five variables: $U(r)$, $P(r)$, $\tilde{E}(r)$, $A(r)$ and $\tilde{\Theta}(r)$, discussed above are associated with four independent field equations (Gergely et al. 2011a; Keresztes & Gergely 2010b), namely,

$$k_4^4 U = \tilde{\Theta}\left(A - \frac{\tilde{\Theta}}{4}\right) + \frac{4\tilde{E}}{3} + \frac{1}{r^2} \quad (29)$$

$$k_4^4 P = \tilde{\Theta}\left(A + \frac{\tilde{\Theta}}{2}\right) - \frac{2\tilde{E}}{3} - \frac{2}{r^2} \quad (30)$$

$$\frac{r\tilde{\Theta}}{2}\tilde{\Theta}' + \frac{\tilde{\Theta}^2}{2} + \frac{4\tilde{E}}{3} + A\tilde{\Theta} = 0 \quad (31)$$

$$\frac{r\tilde{\Theta}}{2}A' + A^2 + \frac{\tilde{\Theta}^2}{4} - \frac{4\tilde{E}}{3} - \frac{1}{r^2} = 0 \quad (32)$$

where prime denotes derivative with respect to the radial coordinate. It is important to note that 31 and 32 involve only variables associated with the brane dynamics. It turns out that in the Schwarzschild scenario, the variables \tilde{E} , $\tilde{\Theta}$ and A can be related in the following way (Gergely et al. 2011a),

$$\frac{2\tilde{E}}{3} + A\tilde{\Theta} = \tilde{\Theta}\left(\frac{\tilde{\Theta}}{4} + A\right) - \frac{1}{r^2} = 0 \quad (33)$$

33 ensures that 31 and 32 coincide and the variables \tilde{E} , $\tilde{\Theta}$ and A are still determined by three equations Gergely et al. (2011a). In the presence of the Weyl fluid, the resultant spherically symmetric metric exhibits a departure from the Schwarzschild spacetime and consequently a modification in 33 is considered,

$$\frac{2\tilde{E}}{3} + A\tilde{\Theta} = M_0\tilde{\Theta}\left(\frac{\tilde{\Theta}}{4} + A\right) - \frac{N_0}{r^2} \quad (34)$$

where M_0 and N_0 are two constant deformation parameters characterizing the Weyl fluid and reducing to 1 in the event the spherically symmetric brane is described by the Schwarzschild solution. 31, 32 and 34 comprises of three equations in the three variables $A(r)$, $\tilde{\Theta}(r)$ and $\tilde{E}(r)$ and the Cauchy-Peano theorem ensures the existence of a solution.

Substitution of 29 and 30 in 34 gives rise to an equation of state connecting the ‘‘dark radiation’’ and the ‘‘dark pressure’’ on the brane,

$$P(r) = (a-2)U(r) - \frac{B}{k_4^4 r^2} \quad (35)$$

where, $M_0 = a/(2a-3)$ and $N_0 = (a-B)/(2a-3)$ such that in the Schwarzschild limit $a = 3$ and $B = 0$. In terms of the reduced variables defined in 2.1, the above equation of state can be rewritten as,

$$p(\mu) = (a-2)\mu - B \quad (36)$$

This equation also serves as a closure condition, which enables us to solve 24 and 25 consistently. The structure of the resultant metric in the brane is discussed in the next section.

Having outlined the procedure by which the 3+1+1 covariant dynamics can be used as a theoretical framework to solve 24 and 25, we now address the consistency of the solution obtained in the brane with that of the bulk. In order to understand the evolution of the various kinematic and gravito-electro-magnetic quantities (mentioned earlier and also discussed in Keresztes & Gergely (2010b)) along the temporal and extra-dimension, one needs to consider the Ricci identities discussed in Keresztes & Gergely (2010b) which are first order differential equations describing the evolution of the aforesaid quantities along the integral curves associated with n^a and u^a . Since we are considering a static scenario, 36 which serves as a boundary condition to be satisfied on the brane at some arbitrary time, continues to hold for all times. On the other hand while considering off-brane evolution, the condition 36 serves as an initial condition to be satisfied on the brane and necessary to solve the first order differential equations describing the evolution along the bulk. The existence of the solution of such differential equations is again guaranteed due to the Cauchy-Peano theorem.

One however needs to ensure that the condition 36 is consistent with the constraint equation on the brane, i.e. $D_\mu E_\nu^\mu = 0$ (given by 12). For a static and spherically symmetric brane 12 simplifies to,

$$\frac{r\tilde{\Theta}}{2}(U + 2P)' + 4AU + P(2A + 3\tilde{\Theta}) = 0 \quad (37)$$

which can be shown to follow from 29-32. Therefore, a static and spherically symmetric background ensures that 37 will always hold true on the brane and hence the initial condition given by 36 is allowed. Hence, the equation of state chosen in this work to close the system of equations 24 and 25, is consistent with the evolution along the bulk. The additional advantage of choosing 36 is that it assumes a simple linear relation connecting the ‘‘dark radiation’’ and the ‘‘dark pressure’’ and can successfully explain the flat rotation curves observed in the galaxies. It turns out that such a choice of the equation of state can also explain the vertical scaleheight data of the LSB galaxies, which we show in the subsequent sections.

2.3 Density profile for the Weyl fluid

Using the equation of state discussed in the last section and ignoring the effect of the cosmological constant, the equation

for the dark pressure 24 can be simplified to ,

$$(2a-3)\frac{d\mu}{d\theta} = -\frac{(a\mu-B)(\tilde{q}+(2a-3)\mu/3-2B/3)}{1-\tilde{q}} + 2\mu(3-a) + 2B \quad (38)$$

while the reduced dark radiation assumes the form,

$$\begin{aligned} \mu(\theta) = & \theta^{2(3-a)/(2a-3)} \exp\left[-\frac{2a}{2a-3} \int v_c^2(\theta) d\theta\right] \times \\ & \left\{ C - \frac{3B}{2a-3} \int [1 + v_c^2(\theta)] \theta^{-2(3-a)/(2a-3)} \times \right. \\ & \left. \exp\left[\frac{2a}{2a-3} \int v_c^2(\theta) d\theta\right] \right\} \end{aligned} \quad (39)$$

where C is an arbitrary integration constant (Gergely et al. 2011b).

In what follows, we will consider the situation where $a \neq 3/2$ and $\tilde{q} \ll 1$. The justification for $\tilde{q} \ll 1$ arises from the fact that a typical galactic dark matter halo has mass $M \approx 10^{12} M_\odot$ and radius $R \approx 100$ kpc, such that $\tilde{q} \approx \frac{Q(r)}{R} \approx 10^{-7} \ll 1$. Since observations reveal that in a galaxy mass is directly proportional to the radius, this ratio remains roughly constant for all galactic radii. The smallness of \tilde{q} further enables us to neglect higher order terms in \tilde{q} , such that 25 assumes the form,

$$\frac{d^2\tilde{q}}{d\theta^2} + m \frac{d\tilde{q}}{d\theta} - n\tilde{q} = b \quad (40)$$

$$m = 1 - \frac{B}{3} - \frac{2}{3} \frac{a(B-3)+9}{2a-3} \quad a \neq \frac{3}{2} \quad (41)$$

$$n = \frac{2}{3} \frac{a(2B-3)+9}{2a-3} \quad a \neq \frac{3}{2} \quad (42)$$

$$b = \frac{2}{3} \frac{B(B-3)}{3-2a} \quad a \neq \frac{3}{2} \quad (43)$$

The general solution of 40 is,

$$\tilde{q}(r) = q_0 + C_1 r^{l_1} + C_2 r^{l_2} \quad (44)$$

where C_1 and C_2 are constants of integration and q_0 is given by,

$$q_0 = -\frac{b}{n} = \frac{B(B-3)}{a(2B-3)+9} \quad (45)$$

while

$$l_{1,2} = \frac{-m \pm \sqrt{m^2 + 4n}}{2} \quad (46)$$

The solution for reduced dark radiation is given by,

$$\mu(r) = q_0 + C_1(1+l_1)r^{l_1} + C_2(1+l_2)r^{l_2} \quad (47)$$

In the original radial coordinate r the solution for dark radiation $U(r)$ is,

$$\rho_h(r) = 3\alpha U(r) = \frac{q_0}{r^2} + C_1(1+l_1)r^{l_1-2} + C_2(1+l_2)r^{l_2-2} \quad (48)$$

which serves as the proxy for the density profile of dark matter.

The dark mass profile is given by,

$$Q(r) = r(q_0 + C_1 r^{l_1} + C_2 r^{l_2}) - 2GM_0 \quad (49)$$

where M_0 is a mass like constant due to the Weyl fluid.

For completeness we also mention that the tangential velocity of a test particle in the ‘dark matter’ dominated region is given by ,

$$v_c^2 \approx v_{c_\infty}^2 + \gamma r^{l_1} + \eta r^{l_2} \quad \text{where,} \quad (50)$$

$$v_{c_\infty}^2 = \frac{1}{3}(aq_0 - B) \quad (51)$$

$$\gamma = \frac{C_1}{2} \left[1 + \frac{(2a-3)}{3}(1+l_1) \right] \quad (52)$$

$$\eta = \frac{C_2}{2} \left[1 + \frac{(2a-3)}{3}(1+l_2) \right] \quad (53)$$

(Gergely et al. 2011a). At this stage, it is important to mention the components of the metric given in 14. The g_{tt} component of the metric can be obtained by solving 15 where the tangential velocity v_c of the test particle is given by 50 which yields,

$$e^{\nu(r)} = C_\nu r^{2\nu_{c_\infty}^2} \times \exp\left[C_1 \frac{3+(2a-3)(1+l_1)}{3l_1} r^{l_1} + C_2 \frac{3+(2a-3)(1+l_2)}{3l_2} r^{l_2} \right] \quad (54)$$

where C_ν is an arbitrary constant of integration. In the outer parts of the galaxy with large radial distances one can approximate $e^{\nu(r)} \approx C_\nu r^{2\nu_{c_\infty}^2}$ (Gergely et al. (2011a)). The g_{rr} component of the metric is given by 20, where $Q(r)$ can be obtained from 49 and contribution of Λ_4 is neglected (discussion in 2.1) such that,

$$e^{-\lambda} = 1 - (q_0 + C_1 r^{l_1} + C_2 r^{l_2}) + \frac{2GM_0}{r} - \frac{C}{r} \quad (55)$$

In order to obtain a flat rotation curve at large distances l_1 and l_2 should be negative. The constrain on the Weyl parameters from the rotation curve has been derived in Gergely et al. (2011b). The goal of this work is to constrain the Weyl parameters from the vertical scale height data of the Low Surface Brightness galaxies (LSBs).

One can show that when $\tilde{q} \ll 1$ and $a \neq 3/2$ the parameters m , n , q_0 and $v_{c_\infty}^2$ can be further simplified such that,

$$m \approx \frac{4a-9}{2a-3}, \quad (56)$$

$$n \approx -2 \frac{a-3}{2a-3}, \quad (57)$$

$$q_0 \approx \frac{B}{a-3} \quad \text{and} \quad (58)$$

$$v_{c_\infty}^2 \approx \frac{a}{3} \left(q_0 - \frac{B}{a} \right) \quad (59)$$

56 and 57 implies that

$$l_1 \approx -1 \quad \text{and} \quad l_2 \approx -1 + \frac{3}{2a-3} \quad (60)$$

which further ensures that a cannot assume values between $3/2$ to 3 . The positivity of $v_{c_\infty}^2$ requires that when $a < 3/2$,

$B \leq 0$ while when $a > 3$, $B > 0$. The density profile for the Weyl fluid assumes the form,

$$\rho_h(r) \approx \frac{q_0}{r^2} + \frac{3C_2}{2a-3} r^{-3(1-\frac{1}{2a-3})} \quad (61)$$

while the rotation curve is given by,

$$v_c^2 \approx \frac{B}{a-3} + \frac{C_1}{2} r^{-1} + C_2 r^{-1+\frac{3}{2a-3}} \quad (62)$$

By taking $C_1 = \frac{2G(M_b+M_U)}{c^2}$ (where $M_U = Q(r)/G$ and M_b here refers to the baryonic mass), $C_2 = Cc^2 R_{c(DM)}^{1-\alpha_{DM}} = -\beta_{DM}$ and by defining $\alpha_{DM} = 3/(2a-3)$ and $\beta_{DM} = B/(a-3)$, the final expressions for the rotation curve and the density profile are given by,

$$\left(\frac{v_c(r)}{c}\right)^2 \approx \frac{G(M_b+M_U)}{c^2 r} + \beta_{DM} \left[1 - \left(\frac{R_{c(DM)}}{r}\right)^{1-\alpha_{DM}}\right] \quad \text{and} \quad (63)$$

$$\rho_h(r) \approx \frac{c^2 \beta_{DM}}{Gr^2} \left[1 - \alpha_{DM} \left(\frac{R_{c(DM)}}{r}\right)^{1-\alpha_{DM}}\right] \quad (64)$$

Due to the constraints on the parameters a and B , it can be shown that either $\alpha_{DM} < 0$ or $0 < \alpha_{DM} < 1$ and $0 < \beta_{DM} \ll 1$ (Gergely et al. 2011b).

It is interesting to compare the Weyl model derived from braneworld gravity with other alternatives to dark matter, e.g. MOND (Modified Newtonian dynamics) (Milgrom 1983). Within the domain of MOND, there exists a universally constant acceleration scale below which the gravitational dynamics deviates significantly from Newton’s laws. The framework of MOND becomes specially relevant in the low acceleration regimes e.g. stars in the outer parts of galaxies such that the model can successfully reproduce the flat rotation curves observed in galaxies without invoking dark matter. The modifications introduced in the laws of gravitation lead to a relation between the asymptotic velocity of galaxies and the total baryonic mass. Such a relation commonly known as the Baryonic Tully Fisher relation entails that the fourth power of the asymptotic velocity of galaxies is proportional to the total baryonic mass.

It may be interesting to investigate the consistency of the rotation curve derived in the Weyl model 63 with the Baryonic Tully Fisher Relation (BTFR) and the Radial Acceleration Relation (RAR) (McGaugh et al. 2000; McGaugh 2012; McGaugh et al. 2016). The Baryonic Tully Fisher Relation (BTFR) states that the fourth power of the asymptotic velocity of galaxies V_f is proportional to the total baryonic mass M_B , i.e.,

$$M_B = AV_f^4 \quad (65)$$

where V_f is obtained from the flat part of the galactic rotation curve. By investigating the mass distribution and the rotation curves of a large number of galaxies with different morphologies, the proportionality constant A was shown to vary between $35 - 50 M_\odot \text{km}^{-4} \text{s}^4$ (McGaugh et al. 2000; McGaugh 2012). This relation can be derived in the deep MOND regime (Milgrom 1983), where the gravitational force F is assumed to be proportional to the square of the acceleration a ,

$$F = \frac{GM_{tot}}{r^2} = \frac{a^2}{g^\dagger} = \frac{1}{g^\dagger} \left(\frac{v^2}{r}\right)^2 \quad (66)$$

where v is the circular velocity at radius r and g^\dagger is considered to be a universally constant acceleration scale such that $a \ll g^\dagger$ defines the deep MOND regime. Thus, if the force law given by 66 is assumed, it can be easily shown that 65 follows from 66. The Radial Acceleration Relation (RAR) proposes that the observed radial acceleration g_{obs} derived from the rotation curve and the baryonic acceleration g_{bar} derived from the observed mass distribution of galaxies obeys the following relation McGaugh et al. (2016),

$$g_{obs} = \frac{g_{bar}}{1 - e^{-\sqrt{g_{bar}/g^\dagger}}} \quad (67)$$

It can be shown from 67 that when $g_{bar} \ll g^\dagger$, $g_{obs} \propto \sqrt{g_{bar}}$ while $g_{obs} \approx g_{bar}$ at high accelerations McGaugh et al. (2016). By analysing data of 153 galaxies from the SPARC database, it was reported that $g^\dagger = 1.2 \pm 0.02$ (random) ± 0.24 (systematic) $\times 10^{-10} \text{m s}^{-2}$ (McGaugh et al. 2016; Lelli et al. 2017).

In what follows we will show that if we assume the BTFR then we can obtain the RAR from the circular velocity profile derived in the Weyl model. It is clear from 63 that at large r , the rotation curve is dominated by the term β_{DM} , i.e. $v_c \approx c\sqrt{\beta_{DM}}$ at the outer part of the galaxy. This parameter which is inherited from the Weyl model is therefore fixed from the flat part of the observed rotation curve of the galaxies, which implies,

$$v_c^2 = V_f^2 = c^2 \beta_{DM} \quad (68)$$

At this point if we assume that the galaxy obeys the BTFR, then from 65 and 68,

$$V_f^4 = \frac{M_B}{A} = c^4 \beta_{DM}^2 \quad (69)$$

This gives a connection between the Weyl parameter β_{DM} with the total baryonic mass of the galaxy, such that,

$$M_B = Ac^4 \beta_{DM}^2 \quad (70)$$

Now, in order to derive the RAR, we rewrite 63 in the following form,

$$\frac{v_c^2}{r} \approx \frac{GM_b}{r^2} + \frac{GM_U}{r^2} + c^2 \beta_{DM} \frac{1}{r} \left[1 - \left(\frac{R_{c(DM)}}{r}\right)^{1-\alpha_{DM}}\right] \quad (71)$$

The left hand side of 71 can be identified with the observed radial acceleration at each radius (g_{obs}) derived from the rotation curve, while the radial acceleration solely due to the baryons is given by $g_{bar} = \frac{GM_b}{r^2}$. This enables us to rewrite 71 in the following form,

$$\begin{aligned} g_{obs} &= g_{bar} + \frac{GM_U}{r^2} + c^2 \beta_{DM} \frac{1}{r} \left[1 - \left(\frac{R_{c(DM)}}{r}\right)^{1-\alpha_{DM}}\right] \\ &= g_{bar} + \frac{g_{bar} M_U}{M_b} + \beta_{DM} c^2 \sqrt{\frac{g_{bar}}{GM_b}} \left[1 - \left(\sqrt{\frac{g_{bar}}{GM_b}} R_{c(DM)}\right)^{1-\alpha_{DM}}\right] \end{aligned} \quad (72)$$

72 can be obtained from 71 by replacing $1/r$ in terms of g_{bar} and M_b . If we assume that $M_U \ll M_b$ (i.e. the core is dominated by the baryons), the second term in 72 can be dropped compared to the other terms.

Further, at large r , M_b becomes equal to the total baryonic mass M_B such that 72 can be written as,

$$g_{obs} = g_{bar} + \sqrt{\frac{g_{bar}}{GA}} \left[1 - \left(\sqrt{\frac{g_{bar}}{GA}} \frac{R_{c(DM)}}{c^2 \beta_{DM}}\right)^{1-\alpha_{DM}}\right] \quad (73)$$

It is important to note that in 73 the quantity $\frac{GAc^4\beta_{DM}^2}{R_{c(DM)}^2}$ defines an acceleration scale. Recalling that $\beta_{DM} \ll 1$ and considering representative values of $\beta_{DM} \approx 10^{-7}$, $R_{c(DM)} \approx 1.5$ kpc and $A \approx 35 M_{\odot}\text{km}^{-4}\text{s}^4$, it can be shown that $\frac{GAc^4\beta_{DM}^2}{R_{c(DM)}^2} \approx 1.76 \times 10^{-10} \text{m s}^{-2}$ which is very close to the universal acceleration scale g^{\dagger} of MOND, where the estimated value of $g^{\dagger} = 1.2 \pm 0.02$ (random) ± 0.24 (systematic) $\times 10^{-10} \text{m s}^{-2}$ (McGaugh et al. (2016)). We further note that α_{DM} has the theoretical constraints, either $\alpha_{DM} < 0$ or $0 < \alpha_{DM} < 1$. Therefore, in the limit, $g_{bar} \ll \frac{GAc^4\beta_{DM}^2}{R_{c(DM)}^2}$ and taking $\alpha_{DM} < 0$, the second term in the square bracket of 73 can be easily dropped compared to unity. Hence, in such a situation 73 reduces to,

$$g_{obs} \approx g_{bar} + \sqrt{\frac{g_{bar}}{GA}} \quad (74)$$

Moreover, considering $A \approx 35 M_{\odot}\text{km}^{-4}\text{s}^4$ (McGaugh et al. (2000)), it turns out that $GA \approx 4.67 \times 10^9 \text{m}^{-1}\text{s}^2$. Since we are in the regime $g_{bar} \ll 10^{-10} \text{m s}^{-2}$, the second term in 74 dominates over the first and we recover the result $g_{obs} \propto g_{bar}^{1/2}$ as expected in the deep MOND regime.

In the event $r \approx R_{c(DM)}$ or $\alpha_{DM} \rightarrow 1$, the term in the square bracket of 72 becomes negligible compared to the first term such that the Newtonian relation $g_{obs} = g_{bar}$ is recovered. This discussion explains that if BTFR is assumed then the RAR can be obtained from the rotation curve derived in the Weyl model. MOND on the other hand predicts the BTFR from the theory once the force law is modified from Newton's law in the low acceleration regime, i.e. $g_{bar} \propto g_{obs}^2$ is assumed as in 66.

We further note that the theoretical constraints on the value of α_{DM} ($\alpha_{DM} < 0$ or $0 < \alpha_{DM} < 1$) makes it easier to reproduce the Radial Acceleration Relation. Had α_{DM} been greater than unity then we would not obtain $g_{obs} \propto g_{bar}^{1/2}$ in the limit $g_{bar} \ll 10^{-10} \text{m s}^{-2}$. Similarly, the requirement $\beta_{DM} \ll 1$ allows the acceleration scale $\frac{GAc^4\beta_{DM}^2}{R_{c(DM)}^2}$ obtained from the Weyl model to be of the same order as the MOND universal acceleration scale. Therefore, the theoretical constraints on the Weyl parameters α_{DM} and β_{DM} are consistent with the predictions of the RAR.

However, the rotation curve cannot be predicted from the observed mass distribution in the braneworld scenario. The density profile presented in 64 corresponds to the density profile of only the Weyl fluid and carries no information about the observed mass distribution. However, if we assume that the galaxy obeys the BTFR then the flat part of the rotation curve which is related to the parameter β_{DM} , can be fixed. However, there are other unknown parameters, e.g. α_{DM} and R_c (72) which can be determined only after fitting the full rotation curve. In this context it is important to mention that MOND predicts the rotation curve Lelli et al. (2017) due to the presence of the universal acceleration scale g^{\dagger} (67).

3 CAN WEYL FLUID ACT AS A PROXY FOR DARK MATTER FOR LSB GALAXIES?

The low surface brightness galaxies (LSBs) are dark matter dominated with negligible baryonic mass such that the ef-

fect of dark matter continues to dominate even in the region where the baryonic disc of stars and gas is present (Gergely et al. 2011a; De Blok et al. 2001; Banerjee et al. 2010; Banerjee & Bapat 2017). In this work however, we do not assume dark matter, but attribute its origin to higher dimensional gravity. Such LSB galaxies have a constant mass density core with core radius of a few kpc (de Blok 2005). Unlike High Surface Brightness (HSB) galaxies, for LSBs we ignore baryonic contribution even within the core radius. Assuming the core radius to be $R_{c(DM)}$ and the mass of the core to be M_{DM} , the constant density of the core is then given by $\rho_{cDM} = \frac{3M_{DM}}{4\pi R_{c(DM)}^3}$.

It therefore follows from 64 that the density profile describing the dark matter in low surface brightness galaxies assumes the form,

$$\rho_{DM}(r) = \frac{3M_{DM}}{4\pi R_{c(DM)}^3} (1 - H_{k_{DM}}(r)) + H_{k_{DM}}(r) \left\{ \frac{c^2 \beta_{DM}}{Gr^2} \left(1 - \alpha_{DM} \left(\frac{R_{c(DM)}}{r} \right)^{1-\alpha_{DM}} \right) \right\} \quad (75)$$

where, $H_{k_{DM}}$ is a smoothing function given by (Gergely et al. 2011a),

$$H_{k_{DM}}(r) = \frac{1}{1 + \exp(-2k_{DM}(r - R_{c(DM)}))} \quad (76)$$

such that it smoothly approaches the Heaviside step function as k_{DM} tends to infinity (Gergely et al. (2011a)), i.e.,

$$H(R_{c(DM)}) = \lim_{k_{DM} \rightarrow \infty} H_{k_{DM}}(R_{c(DM)}) = \begin{cases} 0 & r < R_{c(DM)} \\ 1 & r \geq R_{c(DM)} \end{cases}$$

The purpose of introducing the smoothing function is to ensure that the density distribution of the Weyl fluid changes smoothly from the region of constant density core to the constant rotation curve regime, such that there is no abrupt jump in the energy-momentum tensor of the Weyl fluid across the surface of the core (i.e. no distributional source layer on the surface of the sphere of radius $R_{c(DM)}$). This is necessary, because the metric (given by 14) is the same both inside and outside the core and hence there is no discontinuity in its first derivative. This implies that the extrinsic curvature is continuous across the core and not only the Israel junction conditions but also the Lichnerowicz continuity conditions hold (Gergely et al. (2011a)).

3.1 2-component model of the baryonic disc

We model the galactic baryonic disc as composed of two concentric, co-planar, axi-symmetric discs of stars and atomic hydrogen (HI) gas, which are gravitationally coupled to each other and also in the external force field of a rigid halo of the dark mass. Molecular hydrogen gas H_2 has been neglected in this dynamical model as it is hardly traced in LSBs. In fact, the H_2 to HI mass ratio in late-type LSB spirals is reported to be $\approx 10^{-3}$ (Matthews et al. 2005) and hence can be considered to be a dynamically insignificant component in UGC7321 without significant errors.

The joint Poisson equation in terms of the galactic cylindrical coordinates (R, ϕ, z) is given by

$$\frac{\partial^2 \Phi_{\text{total}}}{\partial z^2} + \frac{1}{R} \frac{\partial}{\partial R} \left(\frac{R \partial \Phi_{\text{total}}}{\partial R} \right) = 4\pi G \left(\sum_{i=1}^2 \rho_i + \rho_{DM} \right) \quad (77)$$

Here, Φ_{total} is the total gravitational potential due to the baryonic disc (stars + gas) and the halo of the dark mass. ρ_i represents the density of the i^{th} component ($i = (\text{stars}), \text{HI}$) and ρ_{DM} is the effective density of the dark mass as given by 75. We note that ρ_{DM} is characterized by five free parameters. Here, the angular term drops off due to the assumed azimuthal symmetry and, similarly, the radial term, for a flat rotation curve. Thus the joint Poisson’s equation reduces to

$$\frac{\partial^2 \Phi_{\text{total}}}{\partial z^2} = 4\pi G \left(\sum_{i=1}^2 \rho_i + \rho_{\text{DM}} \right) \quad (78)$$

We further assume that the stars and HI gas are in vertical hydrostatic equilibrium and also their vertical velocity dispersions remain constant in the z -direction. At a given galacto-centric radius R , the equation of vertical hydrostatic equilibrium for the i^{th} component of the disc ($i = (\text{stars}), \text{gas}$) is given by

$$\frac{\sigma_{z,i}^2}{\rho_i} \frac{\partial \rho_i}{\partial z} + \frac{\partial \Phi_{\text{total}}}{\partial z} = 0 \quad (79)$$

where $\sigma_{z,i}$ the vertical velocity dispersion of the i^{th} component (Rohlfis 1977).

The radial profile of the vertical velocity dispersion of the stars is modelled as

$$\sigma_{z,s}(R) = \sigma_{0s} \exp(-R/\alpha_s R_D) \quad (80)$$

where σ_{0s} and α_s are free parameters. Here σ_{0s} denotes the vertical velocity dispersion of the stars at the centre of the galactic disc; α_s represents the scale length (in units of the exponential disc scale length R_D) with which the vertical velocity dispersion falls off with R . This is closely following van der Kruit (1989) who found that a vertical velocity dispersion of an isothermal, self-gravitating stellar disc should fall off exponentially with radius with a scale length of 2 R_D to match the observed constant stellar scale height in edge-on galaxies.

Similarly, the vertical velocity dispersion of HI has in general been found to either remain constant, or to linearly vary with radius. See, for example, Narayan & Jog (2002). Therefore, we parametrize the vertical velocity dispersion of HI as a polynomial as follows:

$$\sigma_{z,\text{HI}}(R) = \sigma_{0\text{HI}} + \alpha_{\text{HI}} R + \beta_{\text{HI}} R^2 \quad (81)$$

where $\sigma_{0\text{HI}}$, α_{HI} and β_{HI} are free parameters. Here $\sigma_{0\text{HI}}$ is the HI vertical velocity dispersion at the galactic centre.

Therefore, at a given galacto-centric radius R , combining the joint Poisson’s equation and the equation for vertical hydrostatic equilibrium for the i^{th} component we get

$$\frac{\partial^2 \rho_i}{\partial z^2} = -4\pi G \frac{\rho_i}{\sigma_{z,i}^2} (\rho_i + \rho_{\text{DM}}) + \left(\frac{\partial \rho_i}{\partial z} \right)^2 \frac{1}{\rho_i}; \quad (82)$$

Since the stars and gas in the galaxy are mostly concentrated in the galactic disk, it is more natural to express the equations governing their density distributions in cylindrical polar coordinates. However, the vertical density distributions of the stars and gas depend on the density distribution of the dark matter halo ρ_{DM} which has a spherical symmetry (see discussion in 2.1). Since the equations governing the density profiles of baryons (82) are expressed in cylindrical

Table 1. Stellar parameters of UGC 7321 in B-band.

Parameters	UGC7321 ^B
$\mu_0(\text{magarcsec}^{-2})$ ^a	23.5
$\Sigma_0(M_\odot \text{pc}^{-2})$ ^b	34.7
$R_D(\text{kpc})$ ^c	2.1
$h_z(\text{kpc})$ ^d	0.105
M_{stars} ^e	$9.6 \times 10^8 M_\odot$
M_{HI} ^f	$1.1 \times 10^9 M_\odot$

^a Central surface brightness of stellar disk

^b Central surface density of the stellar disk

^c Disc scalelength of the exponential stellar disk

^d Scaleheight (HWHM) of the stellar disk

^e Stellar mass calculated using $2\pi\Sigma_0 R_D^2$

^f HI mass Uson & Matthews (2003)

coordinates but the density profile for the Weyl fluid (75) is expressed in spherical polar coordinates, the spherical radius r (in ρ_{DM}) is expressed in terms of the cylindrical radius R and the vertical height z , in order to solve the two coupled differential equations for stars and gas at every cylindrical radius R .

For a given set of free parameters (M_{DM} , $R_{c(\text{DM})}$, α_{DM} , β_{DM} , k_{DM} , σ_{0s} , α_s , $\sigma_{0\text{HI}}$, α_{HI} , β_{HI}), the above set of two coupled, non-linear, ordinary differential equations (82) in the variables ρ_s and ρ_{HI} is solved iteratively using Runge-Kutta method with initial conditions at mid plane $z = 0$. See, for example, Narayan & Jog (2002) for details. The half-width-at-half-maxima of the density distribution ρ_i at a given R thus obtained is taken to be the scaleheight h_z at that R for that i^{th} component. The set of parameters which gives the best match to the observed stellar and HI scaleheight versus R data defines our best-fitting model.

We use the *Markov Chain Monte Carlo (MCMC)* method for determining the best-fitting set of parameters of our model. We use the task *modMCMC* from the publicly available *R* package *FME* (Soetaert et al. 2010), which implements MCMC using adaptive Metropolis procedure (Haario et al. 2006).

3.2 Input Parameters

UGC 7321 is a prototypical superthin galaxy with a radial-to-vertical axis ratio of 10.3. It is observed at an inclination of 88° and is at a distance of 10 Mpc (Matthews & van Driel 2000; Matthews et al. 1999). The galaxy has a steeply rising rotation curve with an asymptotic velocity of about 110 km s^{-1} (Uson & Matthews 2003).

The de-projected central surface brightness in B-band is $\mu_0 \approx 23.5 \text{magarcsec}^{-2}$ (Matthews et al. 1999). It also has high values of the dynamical mass-to-light ratio with $M_{\text{dyn}}/M_{\text{HI}} = 31$ and $M_{\text{dyn}}/M_{L_B} = 29$, where M_{L_B} is the B-band luminosity, and M_{HI} the total HI mass is the galaxy, M_{dyn} being the dynamical mass of the galaxy. This indicates that the galaxy is dark matter rich as was also corroborated by Banerjee & Jog (2013), who found dark matter dominates the disc dynamics at all radii in this galaxy. Earlier studies have shown

Table 2. Input parameters for HI

Parameters	UGC7321
$\Sigma_{01}(M_{\odot}\text{pc}^{-2})$ ^a	4.912
$\Sigma_{02}(M_{\odot}\text{pc}^{-2})$ ^b	2.50
a_1 (kpc) ^c	3.85
a_2 (kpc) ^d	0.485
r_{01} (kpc) ^e	2.85
r_{02} (kpc) ^f	1.51

- ^a Central surface density of the first HI gaussian disk
^b Central surface density of the second HI gaussian disk
^c Centre of the first HI gaussian disk
^d Centre of the second HI gaussian disk
^e Scalelength of the first HI gaussian disk
^f Scalelength of the second HI gaussian disk

that in the optical i.e., B-band, the surface density profile is well-fitted with an exponential. The same trend holds good for UGC7321 and hence $\Sigma_i(\mathbf{R})$ is given by

$$\Sigma_s(R) = \Sigma_0 \exp(-R/R_D)$$

where $\Sigma_s(0)$ is the central stellar surface density and R_D the exponential stellar disc scalelength. The structural parameters corresponding to the exponential stellar disc of UGC 7321 in B-band were either directly taken or derived from [Uson & Matthews \(2003\)](#).

The HI surface density and the HI scaleheight data for UGC 7321 were obtained from [Uson & Matthews \(2003\)](#) and [O'Brien et al. \(2010\)](#) respectively. Earlier work indicated that the radial profiles of HI surface density could be well-fitted with double-gaussians profiles. See, for example [Begum et al. \(2005\)](#), [Patra et al. \(2014\)](#), possibly signifying the presence of two HI discs. Also, galaxies with the HI surface density peaking away from the centre are common, which indicates the presence of an HI hole at the centre. The HI surface density profiles could be fitted well with off-centred double Gaussians given by

$$\Sigma_{HI}(R) = \Sigma_{01} \exp\left[-\frac{(r-a_1)^2}{2r_{01}^2}\right] + \Sigma_{02} \exp\left[-\frac{(r-a_2)^2}{2r_{02}^2}\right]$$

where Σ_{01} is the central surface density, a_1 the centre and r_{01} the scalelength of gas disc 1 and so on.

The parameters corresponding to stellar disc and the HI disc are summarized in Tables 1 and 2 respectively.

4 RESULTS

Our dynamical model of UGC 7321 in B-band consists of ten free parameters. Out of these, five free parameters correspond to the baryonic disc: σ_{0s} and α_s corresponding to the stellar vertical velocity dispersion profile and σ_{HI} , α_{HI} and β_{HI} corresponding to the HI vertical velocity dispersion profile. The remaining five free parameters are related to the dark mass profile (75) derived from the brane world model: M_{DM} , $R_{c(DM)}$, α_{DM} , β_{DM} uniquely describing the Weyl fluid while k_{DM} is associated with the smoothing function. We use

the observed stellar and HI scaleheight to constrain the ten free parameters described above.

In Figure 1 [Left Panel], we present the vertical velocity dispersion of stars and HI as a function of galacto-centric radius from the 2-component model. We find that the central stellar velocity dispersion is (13.4 ± 0.6) kms^{-1} , which falls off exponentially with a scalelength $(2.1 \pm 0.4)R_D$, R_D being the exponential stellar disc scale length. The central HI vertical velocity dispersion is given by (15.4 ± 0.5) kms^{-1} with $\alpha_{HI} = (-1.3 \pm 0.2)$ $\text{kms}^{-1}\text{kpc}^{-1}$ and $\beta_{HI} = 0.04 \pm 0.02$ $\text{kms}^{-1}\text{kpc}^{-2}$, indicating that it falls off almost linearly with radius. We note that the velocity dispersion of the stars is lower than the HI velocity dispersion. It is, in general, not possible for the stars to have lower dispersion than the gas clouds in which they are formed, as stars are collision-less and hence cannot dissipate energy via collisions. This possibly indicates that the thin disc stars were born in an underlying cold component of the gas with lower values of velocity dispersion ([Patra et al. 2014](#)).

The values of dark matter mass obtained from the model $M_{DM} = (1.3 \pm 0.2) \times 10^9 M_{\odot}$, core radius $R_{c(DM)} = (1.3 \pm 0.2)$ kpc , the parameters describing the Weyl fluid $\alpha_{DM} = -0.4 \pm 0.1$, and $\beta_{DM} = (1.4 \pm 0.2) \times 10^{-7}$, the term associated with smoothing function is given by $k_{DM} = 2.7 \pm 0.3$. The results are summarized in Table 3. We note the the estimated dark mass M_{DM} is consistent with the typical mass of the dark matter in low surface brightness superthin galaxies. The value of M_{DM} is of the order of 10^9 , which is in agreement with the order of magnitude of dark masses of LSBs reported in [Gergely et al. \(2011b\)](#). The core radius $R_{c(DM)}$ is 1.3 kpc ($\sim 0.6 R_D$), possibly indicating that the Weyl fluid has a dense and compact structure. This complies with a previous study by [Banerjee et al. \(2010\)](#) showing UGC7321 has dense and compact pseudo-isothermal dark matter halo. The values of α_{DM} and β_{DM} , which refer to the deviations of the spherically symmetric metric from the Schwarzschild scenario in general relativity, satisfy the condition $\alpha_{DM} < 0$ and $0 < \beta_{DM} < 1$ and are also comparable with the values of the parameter set obtained by [Gergely et al. \(2011b\)](#) for a sample of nine LSBs using the observed rotation curve. However, we note that the value of k_{DM} is of the order of $15-150 \text{ kpc}^{-1}$, for the sample LSBs studied by [Gergely et al. \(2011b\)](#), but for UGC 7321 we find that the value of k_{DM} equals 2.66 kpc^{-1} . This could be possibly attributed to the fact that UGC7321, like some other superthins, has a relatively steeply rising rotation curve compared to LSBs in general ([Banerjee & Bapat 2016](#)).

In Figure 1 [Middle Panel] we have overlaid the scale heights predicted by the 2-component model on the observed scale heights. This confirms that our best-fitting model matches well with the observations. In Figure 1 [Right Panel] we compare the theoretical rotation curve corresponding to the best-fitting parameters of the 2-component model with the observed rotation curve of UGC 7321. The figure illustrates that the theoretical rotation curve obtained by using the best-fitting parameters from the scaleheight constraint on two-component model mostly agrees with the observed rotation curve within error-bars. We note that the rotation curve begins to flatten from ~ 10 kpc and continues to be flat as far as we have available data.

However, we expect galactic dark matter halos to have a finite "size", which should result in a falling rotation curve

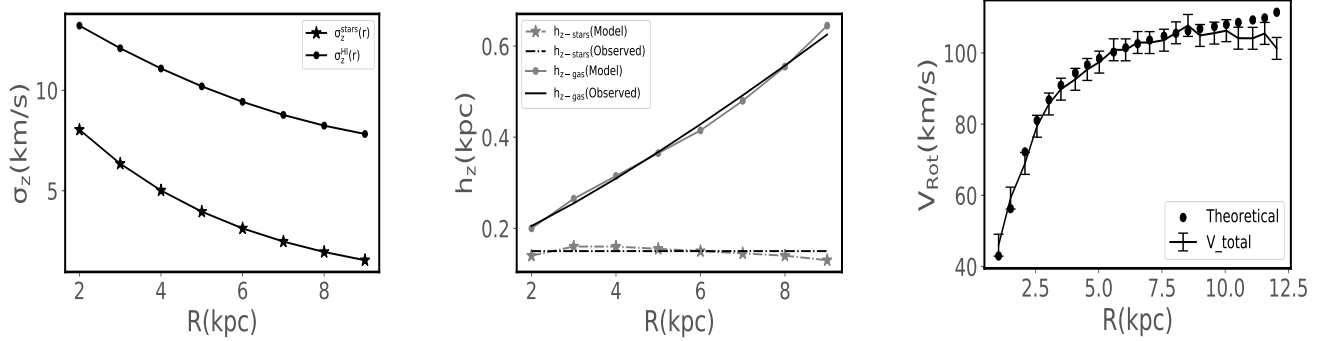


Figure 1. In the Left Panel, we present the vertical velocity dispersion of stars and HI as a function of galacto-centric radius R using ‘stars’ and ‘dots’ respectively, as determined from the 2-component model of the baryonic disc embedded in a halo of dark mass as constrained by the observed stellar and HI scaleheight data. In the Middle Panel, we plot the observed stellar and HI scaleheight with black ‘dash-dot’ and black ‘solid line’ respectively. Overlaid on them is the modelled stellar and HI scaleheight represented by grey ‘stars’ and ‘dots’ respectively. In the Right Panel, we present the rotation curve of UGC 7321 using the best-fit parameters describing the dark matter density profile in the brane-world model and superpose it on the observed rotation curve.

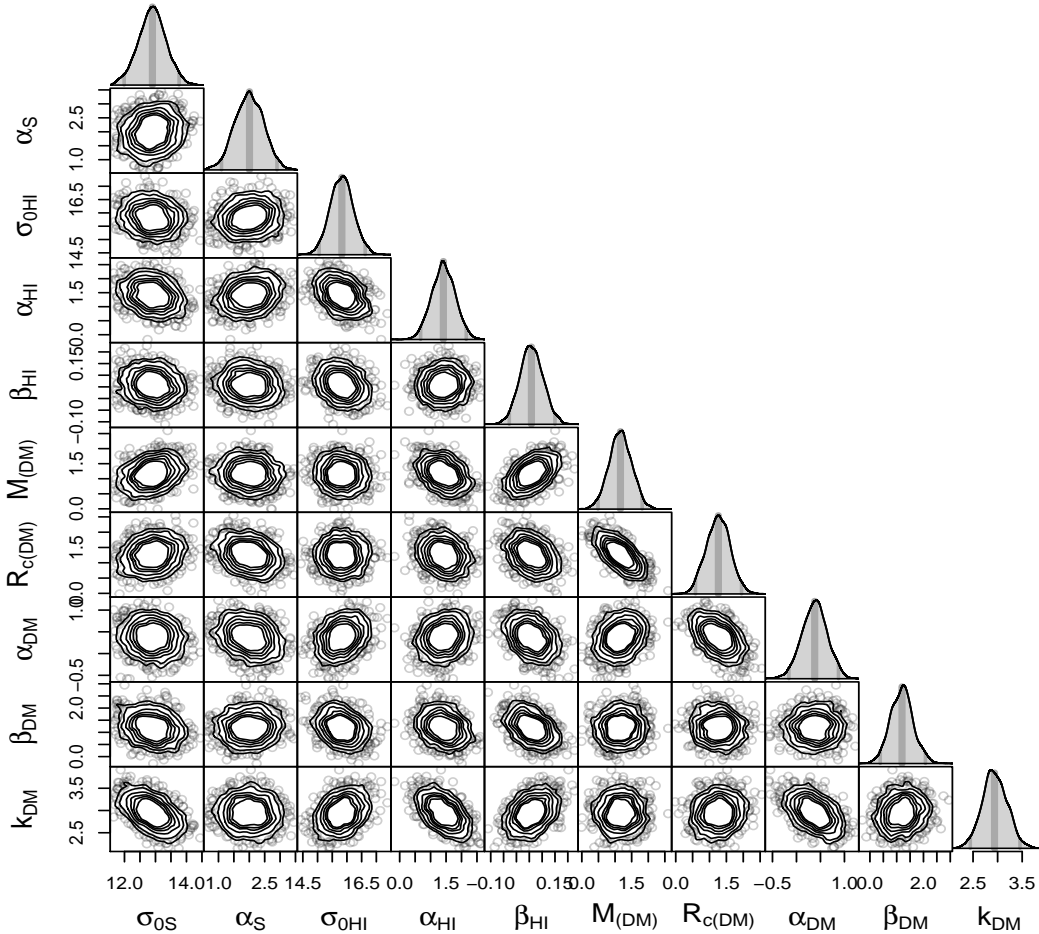


Figure 2. We present the correlation plots and the posterior distributions of the free parameters characterizing the dynamical model of UGC7321 consisting of the 2-component baryonic disc embedded in a halo of dark mass as constrained by the observed stellar and HI scaleheight data using the MCMC method.

Table 3. Best-fit parameters found after optimizing the model

Parameters	UGC7321
σ_{0s} (kms ⁻¹) ^a	13.4 ± 0.6
α_s (kpc ⁻¹) ^b	2.0 ± 0.4
σ_{HI} (kms ⁻¹) ^c	15.4 ± 0.5
α_{HI} (kms ⁻¹ kpc ⁻¹) ^d	-1.3 ± 0.2
β_{HI} (kms ⁻¹ kpc ⁻²) ^e	0.04 ± 0.02
M_{DM} (M_\odot) ^f	(1.3 ± 0.2) × 10 ⁹
$R_{c(DM)}$ (kpc) ^g	1.3 ± 0.2
α_{DM} ^h	-0.4 ± 0.1
β_{DM} ⁱ	(1.4 ± 0.2) × 10 ⁻⁷
k_{DM} (kpc ⁻¹) ^j	2.7 ± 0.3

^a Central stellar vertical velocity dispersion

^b Exponential radial scale length (in units of R_D) of the stellar vertical velocity dispersion

^c Central HI vertical velocity dispersion

^d Radial gradient of HI vertical velocity dispersion

^e Gradient of the radial gradient of HI vertical velocity dispersion

^f Dark mass

^g Core-radius of the dark mass density profile

^h Weyl-fluid parameter

ⁱ Weyl- fluid parameter

^j Smoothing term associated with dark mass density profile

beyond the radius equal to the “size” of the galactic halo. One way to indicate the “size” of the dark matter halo is to consider its virial radius, which is the radius at which the average dark matter density is 200 times the critical density of the universe. For UGC 7321, this is ~ 70 kpc (De Blok et al. 2001; Oh et al. 2008; Lelli et al. 2016). However, with the current observations, there is no way to check if the rotation curve actually falls off beyond the virial radius of the galaxy due to the near-absence of tracer gas at those large radii.

Since we do not have data points of the rotation curve at large galacto-centric radii, the brane-world model parameters are constrained by the observed rotation curve only, which extends upto a radius of about one-tenth of the virial radius of the galaxy. If we extend the rotation curve of UGC 7321 using the best-fitting values of the model parameters (given in Table 3 of the revised version) say upto, ~ 100 kpc, then we note that the curve continues to be flat with no decline. However, this asymptotic behavior is consistent with the pseudo-isothermal dark matter density profile which is routinely used to fit the rotation curves of all galaxies (De Blok et al. 2001; Oh et al. 2008; Lelli et al. 2016).

In Figure (2), we present the correlation plots and the posterior distributions obtained from the MCMC fitting of the 2-component model. Except for a few cases, we do not note strong correlations between the free parameters of the model.

5 SUMMARY AND CONCLUSIONS

In this work, we explore the possibility of higher dimensional gravity in explaining the vertical scaleheight structure of the dark matter dominated LSB galaxy UGC 7321, where the role of dark matter is played by five dimensional

Einstein gravity. The five dimensional Einstein’s equations are projected onto the 3-brane where our visible universe resides such that the effective 4-dimensional gravitational field equations inherits a source term originating from the bulk. The source term owes its origin to the electric part of the bulk Weyl tensor and captures the non-local effects of the bulk onto the brane. For a brane observer therefore, the bulk effectively behaves like a fluid (the so called Weyl fluid) possessing an energy density and pressure, viz, the dark radiation and the dark pressure terms respectively. Due to the presence of the Weyl term, the static, spherically symmetric and asymptotically flat solution of the 4-d effective gravitational field equations deviates from the Schwarzschild spacetime. The degree of deviation from the Schwarzschild scenario is determined by the parameters connecting the dark radiation and the dark pressure terms in the equation of state of the Weyl fluid. The equation of state essentially assigns some initial conditions to the evolution equations of the off-brane quantities (e.g. the normalized normals) along the extra dimensions. In the context of galaxies, it turns out that the appropriate equation of state is $p = (a - 2)\mu - B$, where $a = 3$ and $B = 0$ corresponds to the Schwarzschild scenario. With this equation of state and by employing $\tilde{q} \equiv GM/R \approx 10^{-7} \ll 1$ (which holds true in the galactic situation), one can obtain the density profile and the rotation curve of the LSB galaxies in terms of the equation of state parameters. These are fitted with the available rotation curve and scale height data of UGC 7321 to constrain the Weyl parameters as well as the stellar and HI vertical velocity dispersion profiles. It is important to note that the Weyl model cannot predict the rotation curve from the observed mass distribution since the Weyl parameters are not universal constants. In other words, by fitting the rotation curves and the vertical scale height data of different galaxies we obtain different sets of values for the Weyl parameters within their physically allowed domain.

The rotation curve can be predicted in the premise of MOND due to the universality of the acceleration scale g^\dagger . However, unlike the braneworld model, the physical origin of the universal acceleration scale, the interpolating function between the low and high accelerations or the force law obeyed by particles in the deep-MOND regime is not well understood Milgrom (2015). As far as compliance of MOND with the vertical structure of galaxies is concerned, we may note that Sánchez-Salcedo et al. (2008) studied if the observed HI vertical thickness of the Milky Way could be modelled in the MOND scenario. Using a 2-component galactic disc model of gravitationally-coupled stars and gas, similar to the one studied in this paper, and assuming a constant value of 9 kms⁻¹ for HI vertical velocity dispersion, they found that the model scaleheight fitted the observed scaleheight well at $R > 17$ kpc i.e., beyond 5-6 R_D . However, at $R < 17$ kpc, the model was found to under-predict the observed scaleheight by about 40%.

By fitting the rotation curves of LSB as well as HSB galaxies (Chakraborty & SenGupta 2016; Gergely et al. 2011b) the Weyl parameters have been determined in the past. This motivates us to confront this model with the stellar and HI vertical scale height data of dark matter dominated LSB galaxies, e.g. UGC 7321 which is a very well studied object with a dynamical mass as large as $M_{dyn}/M_{HI} = 31$ and $M_{dyn}/M_{LB} = 29$. Our analysis reveals that the Weyl model

can not only address the observations related to the rotation curve but can also successfully explain the vertical scale-height data of UGC 7321 within the error bars. Therefore apart from the rotation curve, this work opens up a new observational avenue which can be utilized in understanding the role of extra dimensions or other alternative gravity models in the galactic scale.

6 DATA AVAILIBTY

The data underlying this article are available in the article itself

ACKNOWLEDGEMENT

KA would like to thank Prof. T. Harko for useful discussion. IB thanks Sumanta Chakraborty for useful discussions at various stages of this work. AB would like to acknowledge the research grant from DST-INSPIRE Faculty Fellowship (DST/INSPIRE/04/2014/015709) for partially supporting this work. The research of SSG is partially supported by the Science and Engineering Research Board-Extra Mural Research Grant No. (EMR/2017/001372), Government of India. The authors would also like to thank the anonymous referee for insightful comments which have helped improve the quality of the paper.

REFERENCES

Agnese R., et al., 2013, Physical review letters, 111, 251301
 Antoniadis I., 1990, *Phys.Lett.*, B246, 377
 Antoniadis I., Arkani-Hamed N., Dimopoulos S., Dvali G., 1998, *Phys.Lett.*, B436, 257
 Arkani-Hamed N., Dimopoulos S., Dvali G., 1998, *Phys.Lett.*, B429, 263
 Arkani-Hamed N., Dimopoulos S., Dvali G., 1999, *Phys. Rev. D*, 59, 086004
 Arkani-Hamed N., Dimopoulos S., Kaloper N., March-Russell J., 2000, *Nucl. Phys. B*, 567, 189
 Banerjee A., Bapat D., 2016, Monthly Notices of the Royal Astronomical Society, 466, 3753
 Banerjee A., Bapat D., 2017, Monthly Notices of the Royal Astronomical Society, 466, 3753
 Banerjee A., Jog C. J., 2008, The Astrophysical Journal, 685, 254
 Banerjee A., Jog C. J., 2011, The Astrophysical Journal Letters, 732, L8
 Banerjee A., Jog C. J., 2013, Monthly Notices of the Royal Astronomical Society, 431, 582
 Banerjee N., Paul T., 2017, *Eur. Phys. J. C*, 77, 672
 Banerjee A., Matthews L. D., Jog C. J., 2010, New Astronomy, 15, 89
 Banerjee I., Chakraborty S., SenGupta S., 2019, *Phys. Rev. D*, 99, 023515
 Becquaert J.-F., Combes F., 1997, arXiv preprint astro-ph/9704088
 Begum A., Chengalur J. N., Karachentsev I., 2005, Astronomy & Astrophysics, 433, L1
 Binetruy P., Deffayet C., Langlois D., 2000, *Nucl.Phys.*, B565, 269
 Binney J., Tremaine S., 2008, Galactic dynamics. Princeton university press
 Boehmer C., Harko T., 2007, Classical and Quantum Gravity, 24, 3191

Bryan S., Mao S., Kay S., Schaye J., Dalla Vecchia C., Booth C., 2012, Monthly Notices of the Royal Astronomical Society, 422, 1863
 Carlberg R., et al., 1997, The Astrophysical Journal Letters, 485, L13
 Chakraborty S., SenGupta S., 2014, *Phys. Rev. D*, 90, 047901
 Chakraborty S., SenGupta S., 2015, *Eur. Phys. J. C*, 75, 538
 Chakraborty S., SenGupta S., 2016, *Eur. Phys. J.*, C76, 648
 Chakraborty S., Sengupta S., 2014, *Eur. Phys. J. C*, 74, 3045
 Csaki C., Graesser M., Kolda C. F., Terning J., 1999, *Phys.Lett.*, B462, 34
 Csaki C., Graesser M., Randall L., Terning J., 2000, *Phys.Rev.*, D62, 045015
 Davoudiasl H., Hewett J., Rizzo T., 2000a, *Phys. Rev. Lett.*, 84, 2080
 Davoudiasl H., Hewett J., Rizzo T., 2000b, *Phys.Lett.*, B473, 43
 Davoudiasl H., Hewett J., Rizzo T., 2001, *Phys.Rev.*, D63, 075004
 De Blok W., McGaugh S. S., Bosma A., Rubin V. C., 2001, The Astrophysical Journal Letters, 552, L23
 Dienes K. R., Dudas E., Gherghetta T., Riotto A., 1999, *Nucl. Phys. B*, 543, 387
 Famaey B., Binney J., 2005, Monthly Notices of the Royal Astronomical Society, 363, 603
 Fichtel S., 2020, *JHEP*, 04, 016
 Garriga J., Tanaka T., 2000, *Phys.Rev.Lett.*, 84, 2778
 Gentile G., Salucci P., Klein U., Vergani D., Kalberla P., 2004, Monthly Notices of the Royal Astronomical Society, 351, 903
 Gergely L. A., Harko T., Dwornik M., Kupi G., Keresztes Z., 2011a, *Mon. Not. Roy. Astron. Soc.*, 415, 3275
 Gergely L., Harko T., Dwornik M., Kupi G., Keresztes Z., 2011b, Monthly Notices of the Royal Astronomical Society, 415, 3275
 Haario H., Laine M., Mira A., Saksman E., 2006, Statistics and computing, 16, 339
 Haghani Z., Sepangi H. R., Shahidi S., 2012, *JCAP*, 1202, 031
 Harko T., Cheng K., 2006, The Astrophysical Journal, 636, 8
 Harko T., Mak M., 2004, *Phys.Rev.*, D69, 064020
 Horava P., Witten E., 1996, *Nucl.Phys.*, B460, 506
 Hundi R., SenGupta S., 2013, *J.Phys.*, G40, 075002
 Kaluza T., 2018, *Int. J. Mod. Phys. D*, 27, 1870001
 Keresztes Z., Gergely L. A., 2010a, *Annalen Phys.*, 19, 249
 Keresztes Z., Gergely L. A., 2010b, *Class. Quant. Grav.*, 27, 105009
 Klein O., 1926, *Nature*, 118, 516
 Koyama K., 2003, *Phys. Rev. Lett.*, 91, 221301
 Kranz T., Slyz A., Rix H.-W., 2003, The Astrophysical Journal, 586, 143
 Kroupa P., 2012, Publications of the Astronomical Society of Australia, 29, 395
 Kroupa P., 2015, *Can. J. Phys.*, 93, 169
 Lelli F., McGaugh S. S., Schombert J. M., 2016, The Astronomical Journal, 152, 157
 Lelli F., McGaugh S. S., Schombert J. M., Pawlowski M. S., 2017, *Astrophys. J.*, 836, 152
 Lukas A., Ovrut B. A., Waldram D., 2000, *Phys. Rev. D*, 61, 023506
 Maartens R., 2000, *Phys. Rev. D*, 62, 084023
 Maartens R., 2001, in Spanish Relativity Meeting on Reference Frames and Gravitomagnetism (EREs2000) Valladolid, Spain, September 6-9, 2000. ([arXiv:gr-qc/0101059](https://arxiv.org/abs/gr-qc/0101059)), <http://alice.cern.ch/format/showfull?sysnb=2237527>
 Maartens R., 2004a, *Living Rev. Rel.*, 7, 7
 Maartens R., 2004b, Living Reviews in Relativity, 7, 7
 Mak M., Harko T., 2004, Physical Review D, 70, 024010
 Matthews L., van Driel W., 2000, Astronomy and Astrophysics Supplement Series, 143, 421
 Matthews L., Gallagher III J., Van Driel W., 1999, The Astronomical Journal, 118, 2751

- Matthews L. D., Gao Y., Uson J. M., Combes F., 2005, *The Astronomical Journal*, 129, 1849
- Mazumdar A., 2001, *Phys. Rev. D*, 64, 027304
- Mazumdar A., Wang J., 2000, *Phys. Lett. B*, 490, 251
- McGaugh S., 2012, *Astron. J.*, 143, 40
- McGaugh S. S., Schombert J. M., Bothun G. D., de Blok W., 2000, *Astrophys. J. Lett.*, 533, L99
- McGaugh S. S., Rubin V. C., de Blok W., 2001, *The Astronomical Journal*, 122, 2381
- McGaugh S., Lelli F., Schombert J., 2016, *Phys. Rev. Lett.*, 117, 201101
- Milgrom M., 1983, *The Astrophysical Journal*, 270, 365
- Milgrom M., 2015, *Can. J. Phys.*, 93, 107
- Narayan C. A., Jog C. J., 2002, *Astronomy & Astrophysics*, 394, 89
- Navarro J. F., Frenk C. S., White S. D., 1997, *The Astrophysical Journal*, 490, 493
- O'Brien J. C., Freeman K., van der Kruit P., 2010, *Astronomy & Astrophysics*, 515, A62
- Oh S.-H., De Blok W., Walter F., Brinks E., Kennicutt Jr R. C., 2008, *The Astronomical Journal*, 136, 2761
- Oh S.-H., et al., 2015, *The Astronomical Journal*, 149, 180
- Olling R. P., 1996, arXiv preprint astro-ph/9605110
- Patra N. N., Banerjee A., Chengalur J. N., Begum A., 2014, *Monthly Notices of the Royal Astronomical Society*, 445, 1424
- Pawlowski M. S., Famaey B., Merritt D., Kroupa P., 2015, *The Astrophysical Journal*, 815, 19
- Peebles P., Nusser A., 2010, *Nature*, 465, 565
- Polchinski J., 1998
- Rahaman F., Kalam M., DeBenedictis A., Usmani A., Ray S., 2008, *Monthly Notices of the Royal Astronomical Society*, 389, 27
- Randall L., Sundrum R., 1999a, *Phys.Rev.Lett.*, 83, 3370
- Randall L., Sundrum R., 1999b, *Phys.Rev.Lett.*, 83, 4690
- Rohlf K., 1977
- Rubin V., Ford Jr W., Roberts M., 1979, *The Astrophysical Journal*, 230, 35
- Sánchez-Salcedo F., Saha K., Narayan C., 2008, *Monthly Notices of the Royal Astronomical Society*, 385, 1585
- Sanders R., Noordermeer E., 2007, *Monthly Notices of the Royal Astronomical Society*, 379, 702
- Sanders R. H., Verheijen M., 1998, *The Astrophysical Journal*, 503, 97
- Shiromizu T., Maeda K.-i., Sasaki M., 2000, *Phys.Rev.*, D62, 024012
- Soetaert K., Petzoldt T., et al., 2010, *Journal of Statistical Software*, 33, 1
- Sofue Y., Rubin V., 2001, *Annual Review of Astronomy and Astrophysics*, 39, 137
- Uson J. M., Matthews L., 2003, *The Astronomical Journal*, 125, 2455
- Wiseman T., 2002, *Phys. Rev. D*, 65, 124007
- Zwicky F., 1933, *Helvetica physica acta*, 6, 110
- Zwicky F., 1937, *The Astrophysical Journal*, 86, 217
- de Blok W., 2005, *The Astrophysical Journal*, 634, 227
- de Blok W., McGaugh S., 1998, *The Astrophysical Journal*, 508, 132
- de Blok W., Walter F., Brinks E., Trachternach C., Oh S., Kennicutt Jr R., 2008, *The Astronomical Journal*, 136, 2648
- van der Kruit P., 1989, in , *The World of Galaxies*. Springer, pp 256–275